



Finite element solution of conjugate heat transfer problems with and without the use of gap elements

Conjugate heat transfer problems

81

W. Song and B.Q. Li

School of Mechanical and Materials Engineering, Washington State University, Pullman, Washington, USA

Received February 2001

Revised October 2001

Accepted October 2001

Keywords Finite elements, Heat exchangers, Heat transfer

Abstract This paper describes the finite element solution of conjugate heat transfer problems with and without the use of gap elements. Direct and iterative methods to incorporate gap elements into a general finite element program are presented, along with their advantages and disadvantages of the two gap element treatments in the framework of finite elements. The numerical performance of the iterative gap element treatment is discussed in detail in comparison with analytical solutions for both 2- and 3-D gap conductance problems. Numerical tests show that the number of iterations depends on the non-dimensional number $Bi = hL/k$, and it increases approximately linearly with Bi for $Bi \geq 0.6$. Here, for gap heat transfer problems, h is taken to be the inverse of the contact resistance. This conclusion holds true for both 2- and 3-D problems, for both linear and quadratic elements and for both transient and steady state calculations. Further numerical results for conjugate heat transfer problems encountered in heat exchanger and micro chemical reactors are computed using the gap element approach, the direct numerical simulations and analytical solutions whenever solvable. The results reveal that for the standard heat exchanger designs, an accurate prediction of temperature distribution in the moving streams must take into consideration the radial temperature distribution and the accuracy of the calculations depends on the non-dimensional number $Bi = hR/2k$. From gap element calculations, it is found that classical analytical solutions are valid for a heat transfer analysis of an exchanger system, only when $Bi < 0.1$. This important point so far has been neglected in virtually all the textbooks on heat transfer and must be included to complete the heat transfer theory for heat exchanger designs. Results also suggest that for thermal fluids systems with chemical reactions such as micro fuel cells, the gap element approach yields accurate results only when the heat transfer coefficient that accounts for the chemical reactions is used. However, when these heat transfer coefficients are not available, direct numerical simulations should be used for an accurate prediction of the thermal performance of these systems.

Nomenclature

C_p	= heat capacity	L	= length
h	= heat transfer coefficient	\mathbf{P}	= discretized nodal pressure array
\hat{i}, \hat{j}	= unit vectors of the i th, j th components	Q	= volumetric heat source
k	= thermal conductivity	r	= radius

The partial support of this work by NASA (Grant Nos.: NAG8-1477 and NAG8-1693) is gratefully acknowledged.

HFF 12,1	T, \mathbf{T}	= temperature, discretized temperature	ν	= kinematic viscosity
	\mathbf{u}, \mathbf{U}	= velocity, discretized velocity	$\partial\Omega$	= boundary of computational domain
82	x, y	= dimensionless coordinates	∇	= gradient operator
	<i>Greek</i>			
	α	= thermal diffusivity	ρ	= density
	β	= thermal expansion coefficient	Ω	= computational domain
	δ_{ij}	= delta function	<i>Subscripts</i>	
	ϕ	= shape function for velocity	i, j	= the i th, j th point
	θ	= shape function for temperature and concentration	n	= the n th component
	ψ	= shape function for pressure	<i>Superscripts</i>	
	μ	= dynamic viscosity	i, j	= the i th, j th component
			T	= matrix transpose

Introduction

Many thermal and fluid flow systems involve conjugate heat transfer between solids and moving fluids. Accurate prediction of temperature distribution in both the solids and liquids in these systems is of critical importance for a fundamental understanding of the physics governing the thermal and fluid flow processes and for practical system design and optimization. When detailed thermal and fluid flow distributions are required, the thermal balance and the Navier–Stokes equations must be solved, along with appropriate flow and thermal boundary conditions along the solid–liquid interface. Falling into this category are the thermal entrance problems, many microscale thermal and flow problems, novel microelectronic cooling designs involving microscale oscillating jets and nanostructure heat transfer applications (Srinivas and Fletcher, 1992; Cebeci and Bradshaw, 1989; Tannehill *et al.*, 1997; Gartling and Reddy, 1994; LeBounty *et al.*, 1999; Narumanchi *et al.*, 2000). On the other hand, for many other thermal systems in use today, the detailed thermal characteristics and fluid flow structure near the solid–liquid interface are not required in order to obtain a reasonably good representation of thermal performance from the design point of view. For these systems, the heat transfer between the solid and liquid are approximated by a lumped heat transfer coefficient, and in many cases, a plug flow field is used. Notable examples of this type include the macroscale heat exchangers where the overall heat transfer coefficient is used to eliminate the need for the detailed calculations of the temperature distributions in the solid separator dividing the two fluid streams of different temperatures. Classified into this class of problems are also the metal casting processes where the heat transfer through the gap between the solidifying metal and the mold is characterized by a heat conductance and the metal forging processes where heat transfer occurs between the contact surfaces of the mold and workpiece.

The procedures for predicting the performance of conjugate heat transfer by solving the complete thermal balance and Navier–Stokes equations have been well established, thanks to the research effort of past several decades on

numerical development (Gartling and Reddy, 1994; Rule *et al.*, 2000). Criteria for mesh arrangement and accuracy as well as benchmark problems are documented (Davis, 1983). However, there appears to have been very limited work, if any, on the use of gap elements to model the gap heat transfer and the temperature distributions in the regions enclosing the gap. The computational procedures and numerical performance of the gap elements as applied to thermal calculations have not yet been reported for thermal and fluid flow systems. This is particularly true for the case where the nodes across the gap regions are not coincident. Gap elements have been used successfully in modeling mechanic contact problems in the framework of finite elements using the popular Lagrangian multiplier method or the penalty approaches (Bathe and Chaudhary, 1984; Stadler and Weiss, 1979) and have continued to attract a great deal of attention among researchers (Landenberger and El-Zafrany, 1999; Choi and Chung, 1996). The concepts and methodology used in the solid mechanics, although not directly applicable, should be useful in developing the procedures for heat transfer calculations. The numerical development for gap heat transfer calculations of course is not a direct copy of the established numerical implementation of what has been proved successful in solid mechanics for contact problems, because of the unique characteristics of heat transfer involving moving fluids and solids. This is also because unlike the contact problems, the two opposite sides across a gap are never in contact from the heat transfer point of view.

The objective of this paper is two-fold:

- (1) to present a numerical procedure for incorporating into the existing finite element programs the gap elements as applied to conjugate heat transfer, and
- (2) to assess the accuracy and applicability of gap elements for conjugate heat transfer calculations.

While the thrust for the former comes from the desire to establish a systematic approach for conjugate heat transfer problems, the latter is derived from the need to develop a clear understanding of basic assumptions in the simplified approach commonly taken for macroscale heat exchanger problems and to determine under what conditions these assumptions start to break down. The importance of the latter can not be overemphasized, especially in light of the urgent demand to develop optimal procedures for manufacturing microscale thermal MEMS devices, which have recently merited a great deal of attention. In assessing numerical performance, issues of accuracy and applicability of the gap elements in modeling the conjugate heat transfer problems must also be addressed. These issues apparently are best investigated in comparison with the complete solutions of thermal and fluid flow fields. Numerical results computed by the gap element formulation below have led to important findings that go far beyond just the numerical performance issues. Indeed, for some widely performed

calculations for heat exchanger designs, computed results with gap elements suggest that additional assumptions and conditions, other than those already documented in standard textbooks, must be satisfied if the simplified approach is to yield consistent and accurate results.

In what follows, the finite element solution of the conjugate heat transfer problems with and without the use of gap elements is presented. Both two dimensional and three dimensional cases are considered. Two types of gap element treatments based on direct and iterative approaches and their merits and disadvantages are described. Numerical implementation and performance of gap elements used for heat transfer calculations are discussed. Conjugate heat transfer problems are studied comparatively using the formations with and without use of gap elements. The information reported in this study should be of great value not only in developing a systematic computational methodology for conjugate thermal calculations, but also in developing more accurate criteria for heat exchanger design and analysis.

Problem statement

Let us consider two types of problems describing heat transfer between two fluid streams, as illustrated in Figure 1. In Case (a), the fluids of different temperatures moving in the two channels are divided by a solid separator of finite thickness. The no slip conditions are required along the interface between the solid and fluid. The temperature and the heat flux is continuous across the fluid–solid interface. For the sake of illustration, the counter flow configuration is considered. The computational procedures and analyses, of course, are applicable to a concurrent flow configuration as well. In Case (b), the conjugate heat and flow problem as described in Case (a) is simplified such that the separator is replaced by a gap and the detailed features of heat transfer between the two streams divided by the separator are lumped into an overall heat transfer coefficient. This simplification is quite often made in heat exchanger designs (Incropera and DeWitt, 1996; Mills, 1999). The heat transfer between the two streams is therefore characterized by a Newton cooling form, that is, the heat flux is equal to the lumped overall heat transfer coefficient times the difference of the temperatures of the two streams. The governing equations for both cases are the same as below:

$$\nabla \cdot \mathbf{u}_i = 0 \quad (1)$$

$$\rho_i \frac{\partial \mathbf{u}_i}{\partial t} + \rho_i (\mathbf{u}_i \cdot \nabla) \mathbf{u}_i = -\nabla P_i + \eta_i \nabla^2 \mathbf{u}_i \quad (2)$$

$$\rho_i C_{p,i} \frac{\partial T_i}{\partial t} + \rho_i C_{p,i} \mathbf{u}_i \cdot \nabla T_i = \kappa_i \nabla^2 T_i \quad (3)$$

where the subscript i ($i = 1, 2, 3$) refers to fluids 1 and 2 and separator, respectively, and for simplicity only constant properties are considered, although the numerical code used has no such restrictions. When the above equation is applied to the separator, the velocity is set to zero. The boundary conditions are standard, that is, a no-slip condition on the solid, and temperature and heat flux being continuous across the interface, for the conjugate problem as stated in Case (a). Those for Case (b) differ along the gap boundary where the heat transfer is given by,

$$-\kappa_1 \mathbf{n}_1 \cdot \nabla T_1 = h(T_1 - T_2) = \kappa_2 \mathbf{n}_2 \cdot \nabla T_2 \quad (4)$$

Note that the above equations and boundary conditions are applicable to both 2- and 3-D problems. The gap heat transfer coefficient h , which sometimes is called gap conductance, is a function of other variables such as pressure and surface morphology of the gap boundaries.

Finite element formulation

The governing equations for the thermal and fluid flow fields along with the boundary conditions are solved using the Galerkin finite element method. Since details are well documented in many textbooks, only an outline is given here. In essence, the computational domain is first discretized into small elements. Within each element, the dependent variables \mathbf{u} , P and T are interpolated by shape functions of ϕ , ψ and θ :

$$u^i(x, t) = \phi^T U^i(t) \quad (5)$$

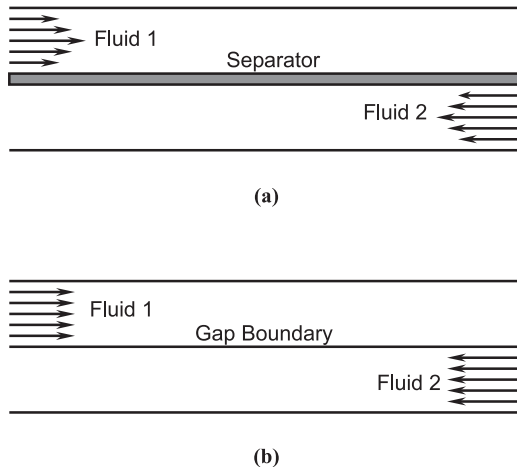


Figure 1. Schematic representation of conjugate heat transfer problems: (a) direct numerical simulation when detailed flow structure near the separator is to be resolved, and (b) the detailed boundary layer near the solid separator is lumped into an overall heat transfer coefficient and the flow is simplified to be a plug flow

$$P(x, t) = \psi^T P(t) \quad (6)$$

$$T(x, t) - T_r = \theta^T T(t) \quad (7)$$

where U^i , \mathbf{P} and \mathbf{T} are column vectors of element nodal point unknowns.

With the above equations substituted into the governing equations, we get the residuals R_1 , R_2 and R_3 which represent the momentum, mass conversion and energy equations respectively. The Galerkin form of the Method of Weighted Residuals seeks to reduce these residuals to zero by making them orthogonal to the weighting functions, which are chosen to be the same as the shape functions. Following the standard procedures given in Gartling and Reddy (1994), the governing equations for the fluid flow and heat transfer are re-written in the following integral form,

$$\left(\int_{\Omega_1} \psi (\hat{i} \cdot \nabla \phi^T + \delta_{2i} \phi^T / r) dV \right) U^i = -\varepsilon \left(\int_{\Omega_1} \psi \psi^T dV \right) P \quad (8)$$

$$\begin{aligned} & \left(\int_{\Omega_1} \rho \phi \phi^T dV \right) \frac{dU^i}{dt} + \left(\int_{\Omega_1} \rho \phi u \cdot \nabla \phi^T dV \right) U^i \\ & - \left(\int_{\Omega_1} (\hat{i} \cdot \nabla \phi + \delta_{2i} \phi / r) \psi^T dV \right) P \\ & + \left(\int_{\Omega_1} \eta (\nabla \phi \cdot \nabla \phi^T + 2\delta_{2i} \phi \cdot \phi^T / r^2) dV \right) U^i + \left(\int_{\Omega_1} \eta (\hat{i} \cdot \nabla \phi) (\hat{j} \cdot \nabla \phi^T) dV \right) U^j \\ & = \int_{\partial \Omega_1} \mathbf{n} \cdot \bar{\sigma} \cdot \hat{i} \phi ds \end{aligned} \quad (9)$$

$$\begin{aligned} & \left(\int_{\Omega_1} \rho C_p \theta \theta^T dV \right) \frac{dT}{dt} + \left(\int_{\Omega_1} \rho C_p \theta u \cdot \nabla \theta^T dV \right) T \\ & + \left(\int_{\Omega_1} k \nabla \theta \cdot \nabla \theta^T dV \right) T = - \int_{\partial \Omega_1} q_T \theta ds \end{aligned} \quad (10)$$

Once the form of shape functions ϕ , θ , and ψ is specified, the integrals defined in the above equations can be expressed by the matrix equation. The momentum and energy equations may be combined into a single global matrix equation:

$$\begin{aligned}
& \begin{bmatrix} M & \mathbf{0} \\ \mathbf{0} & N_T \end{bmatrix} \begin{bmatrix} \dot{U} \\ \dot{T} \end{bmatrix} + \begin{bmatrix} A(U) + K + \varepsilon_p E M_p^{-1} E^T & \mathbf{0} \\ \mathbf{0} & D_T(U) + L_T \end{bmatrix} & \text{Conjugate heat} \\
& \times \begin{bmatrix} U \\ T \end{bmatrix} = \begin{bmatrix} \mathbf{F} \\ \mathbf{G}_T \end{bmatrix} & \text{transfer} \\
& & \text{problems} \\
& & \text{(11)} \quad \underline{\underline{87}}
\end{aligned}$$

In constructing the above matrix equation, the penalty formulation has been applied, and \mathbf{P} in the momentum equation is substituted by:

$$\frac{1}{\varepsilon_p} \mathbf{M}_p^{-1} \mathbf{E}^T \mathbf{U}.$$

The coefficient matrices in the above equation are calculated by:

$$M_p = \int_{\Omega_1} \psi \psi^T dV;$$

$$N_T = \int_{\Omega_1} \rho C_p \theta \theta^T dV$$

$$M = \int_{\Omega_1} \theta \theta^T dV;$$

$$E_i = \int_{\Omega_1} (\hat{i} \cdot \nabla \phi + \delta_{2i} \phi / r) \psi^T dV$$

$$L_T = \int_{\Omega_1} k \nabla \theta \cdot \nabla \theta^T dV;$$

$$A(U) = \int_{\Omega_1} \rho \phi u \cdot \nabla \theta^T dV$$

$$D_T(U) = \int_{\Omega_1} \rho C_p \theta u \cdot \nabla \theta^T dV;$$

$$G_T = - \int_{\partial \Omega_1} q_T \theta ds$$

$$F = \int_{\partial\Omega_1} \phi \tau n ds$$

$$K_{ij} = \left(\int_{\Omega_1} \eta (\nabla \phi \cdot \nabla \phi^T + 2\delta_{2i} \phi \cdot \phi^T / r^2) dV \right) \delta_{ij} + \int_{\Omega_1} \eta (\hat{i} \cdot \nabla \phi) (\hat{j} \cdot \nabla \phi^T) dV$$

where \mathbf{U} is a global vector containing all nodal values of velocity components u , v and w . The assembled global matrix equations are stored in the skyline form and solved using the Gaussian elimination method. The successive substitution method is applied for non-linear iteration, and the time derivatives are approximated using the implicit finite difference scheme, with automatic time step control. The above formulations were explicitly written for problems with axisymmetry, such as pipe flow and heat transfer. With $\delta_{2i} = 0$, the above formulations are applicable to both 2-D ($i = 1,2$) and for 3-D ($i = 1,2,3$) problems.

Treatments of gap elements

Two treatments are differentiated for the use of the gap elements in the finite element solution of conjugate heat transfer problems, depending on the arrangement of the nodes on the opposite sides of a gap.

Direct method

In the first treatment, the nodes across the gap formed by the two adjacent bodies are constructed with such a constraint that the nodes match on a one-to-one basis, as appear in Figure 2a. The formulation for this case is relatively straightforward and the calculation requires no iteration for a linear conduction problem. The mesh generation, though, is somewhat tedious and could perturb the existing mesh generation problem to some extent, because it is necessary to account for both sides across the gap. Taking the linear element as an example, the finite element formulation for the heat flux on side one of the gap by this treatment may be described below:

$$\begin{aligned} \int \theta h (T_1 - T_2) dS &= \int h \theta \theta^T \begin{pmatrix} T_1^1 \\ T_1^2 \end{pmatrix} T_1 - \theta^T \begin{pmatrix} T_1^1 \\ T_1^2 \end{pmatrix} dS \\ &= \begin{bmatrix} a_{11} & a_{12} & b_{11} & b_{12} \\ a_{21} & a_{22} & b_{21} & b_{22} \end{bmatrix} \begin{pmatrix} T_1^1 \\ T_1^2 \\ T_2^1 \\ T_2^2 \end{pmatrix} \end{aligned} \quad (15)$$

where $\theta^T = (0.5(1 - \xi), 0.5(1 + \xi))$, $a_{ij} = \int h \theta_i \theta_j dS$ and $b_{ij} = - \int h \theta_i \theta_j dS$.

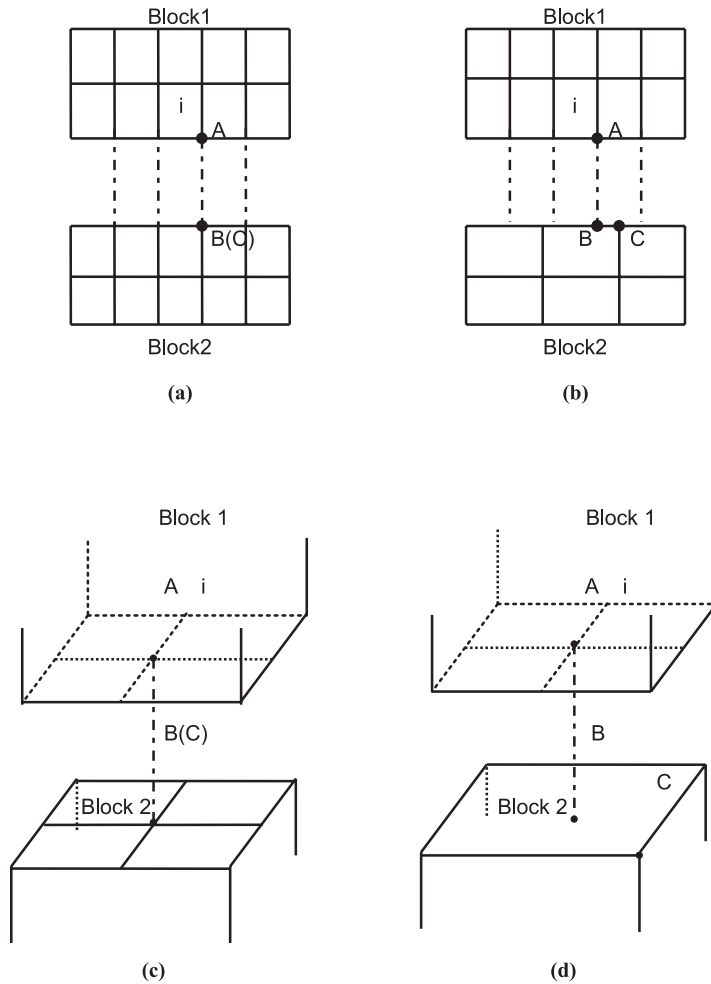


Figure 2. Illustration of two different treatments of gap elements for finite element solutions of conjugate heat transfer problems: (a) and (b) for 2-D problems and (c) and (d) for 3-D problems

Similarly, an elemental matrix may be constructed for the heat flux along the opposite side of the gap. These elemental matrices are then assembled into the global finite element matrix to obtain the final solution. For most finite element programs, however, a more convenient practice would be to perform the above calculations on both sides at the same time and form a combined elemental matrix, which is then incorporated into the global matrix. Apparently, the above formulations can be directly extended to the higher order elements and to 3-D gap elements.

The advantage of the above approach is that it is intuitive and easy to apply and requires no iteration if the heat transfer coefficient is not temperature

dependent. There are, however, several drawbacks associated with this approach. First, it is very difficult to incorporate the above formulation into a commercial finite element package, because of the inaccessibility of the source code. This is important in that many commercially available codes do not have this feature, despite the fact it is simple to apply. Another, yet more serious, drawback of this approach is that it fails when the nodes on the two sides between the gap do not have one-to-one correspondence, as shown in Figure 2b and d. In many engineering calculations, different nodes (or node distributions) are applied in the two different regions embracing the gap to maximize the computational efficiency. There are also situations in which the corresponding nodes are not at the same geometric locations, even although the total number of nodes is the same on both sides of a gap. These arise frequently when an adaptive algorithm is applied. Dislocated nodes also occur in moving boundary problems such as metal forging where the nodes on the one side of the gap slide during each time step while those on the other side remain stationary. To solve these problems, we apply an iterative procedure for incorporating the gap elements, as described below.

Iterative method

Referring to Figure 2b and d, we consider a general case where the two nodes (A and C) are not along the line perpendicular to the two opposite sides and going through A. Thus when the heat flux along element i is considered, the temperature at the corresponding geometric point at the opposite side is required. To locate this point, a straight line, i.e. $A\bar{B}$, is drawn perpendicular to both sides and is passing through the nodal point (i.e. A) under consideration. The intercept of this straight line and the boundary element (i.e. element j) on the opposite side gives the needed geometric coordinates, with which the temperature at the point can be determined by interpolating the temperatures at the nodes of the element. The procedures for interpolation and related formulas for both 2- and 3-D cases are given in the Appendix.

The algorithm for the calculations may now be described. To calculate the heat flux on a gap element, the geometrically corresponding points on its opposite side (e.g. Point B in Figure 2b and d) are determined by searching through all boundary elements on the opposite side and their temperatures are interpolated from the boundary elements that they are associated with. The search algorithm in part is similar to that used to determine the shadowing effects for surface radiative exchange calculations. Once the temperatures are known by interpolation, the heat flux is then calculated as described in the standard finite element formulation,

$$\int \theta h(T_1 - T_2) dS = \int h \theta \left(\begin{matrix} T_1^1 \\ T_1^2 \end{matrix} \right) T_1 - \theta T_B dS$$

$$= \begin{bmatrix} a_{11} & a_{12} \\ a_{21} & a_{22} \end{bmatrix} \begin{pmatrix} T_1^1 \\ T_1^2 \end{pmatrix} - \begin{pmatrix} F_1 \\ F_1 \end{pmatrix} \quad (16)$$

where $F_1 = \int \theta_i T_B dS$. Note that in actual integration, T_B corresponds to the value at the integration point and thus may involve several different elements on the opposite side of an element being considered. The above equation can then be readily incorporated into the global matrix. As the temperature at Point B is not directly solved as a component of the unknown vector and has to be interpolated from the solutions, the process is iterative even for a linear heat transfer problem.

Results and discussion

In this section, a few numerical examples are provided to illustrate the usefulness of the above formulations for conjugate heat transfer calculations. While both gap element formulations are incorporated into the finite element program used for the calculations to follow and are tested against available data, the focus is on the second method because of its unrestricted applications.

Testing with analytical solutions

The finite element formulation with the second gap element treatment is first tested against analytical solutions. Both 2- and 3-D calculations were carried out for the heat transfer through a gap between the two blocks with constant properties and at different temperatures, as appears in the insert of Figure 3. Tests were also performed for linear and higher order elements of both 2- and 3-D. The temperature distribution in the two blocks is plotted in Figure 3, along with analytical solutions. Excellent agreement exists between the numerical and analytical solutions, validating the code development. It is noted here that the problem itself is 2-D but it serves a good testing base against which both 2- and 3-D gap element calculations are checked. Figure 4 shows the number of iterations required for convergence (relative tolerance is set at 1×10^{-5}). Apparently, the convergence rate is a strong function of dimensional parameter group ($Bi = hL/k$) characterizing the heat transfer across the gap. For most engineering applications, hL/k lies between 0.01 and 18 (Incropera and DeWitt, 1996). The tested results are calculated using the simple back substitution method. A higher convergence rate is possible with the Newton–Raphson method. It is worth noting that because the problem is linear, the equal-nodes gap element formulation would require no iterations at all. Numerical experience with these test problems also showed that the same number of

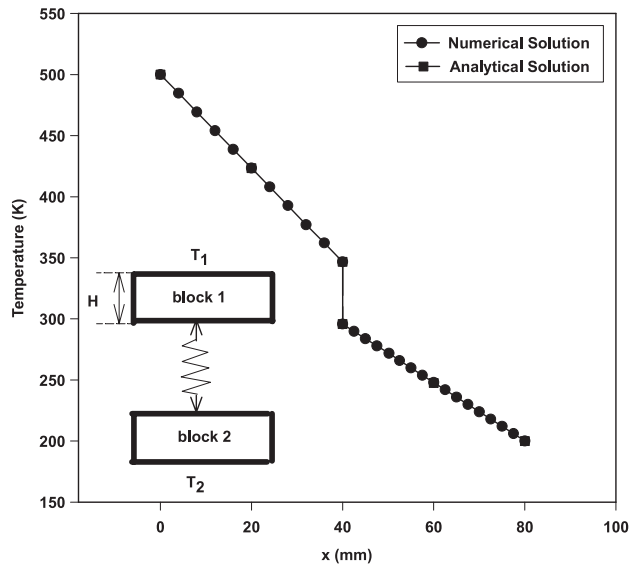
iterations is required for both equal-nodes and unequal-nodes meshes when the iterative formulation is applied. Our tests included a variety of mesh distributions and many different types of elements. Both accuracy and number of required iterations are not sensitive to the mesh distributions and types of elements used, linear or quadratic. Also, numerical results show that the same conclusion holds true for all 2-D, axisymmetric and 3-D cases tested.

The computer code is also capable of performing transient calculations. Some computed results are given in Figure 5 for the transient gap heat transfer for the above configuration by assuming that the two blocks are initially at 300 K and subject to the boundary conditions at $t > 0$. The calculations used an implicit time difference scheme. The number of iterations with gap elements is found to be the same for very time step. It is apparent from the results that for the problem under consideration, the temperature in both blocks reaches a quasi-steady state in a period of 20 s.

Heat exchanger problems

Perhaps, one of the most important applications of gap elements is in the prediction of heat exchanger performance. The textbook treatment of heat transfer between two streams in a heat exchanger is to formulate the heat flux using an overall heat transfer coefficient and the temperature difference between the two streams. The formula is very similar to the gap heat transfer description (equation (4)). We consider the case as shown in the insert of Figure 6, where two fluid streams move in the opposite directions in a concentric pipe.

Figure 3. Comparison of numerical results with analytical solutions for gap conduction problems. Parameters used for computation: thermal conductivity (k) = 148 W/m-K for the top block and thermal conductivity (k) = 237 W/m-K for the bottom block. $L = H = W = 40$ mm for both blocks. Gap conductance (h) = 11,080 (W/m²-K). $Bi = hL/k = 1.87$. The top surface is fixed at 500K and the bottom at 200K



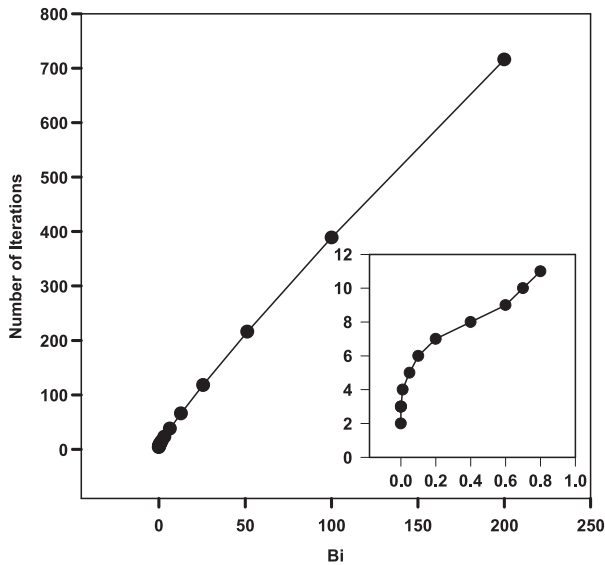


Figure 4. Number of iterations versus $Bi = hH/k$ for convergence using the second treatment of gap elements

The thermophysical properties and the overall heat transfer coefficients are assumed constant for the sake of simplicity. For this problem, the analytical solution is obtained by assuming that the temperatures of two streams are constant in the radial direction. Also, the overall heat transfer coefficient includes the effect of the separator dividing the two streams, assuming that the

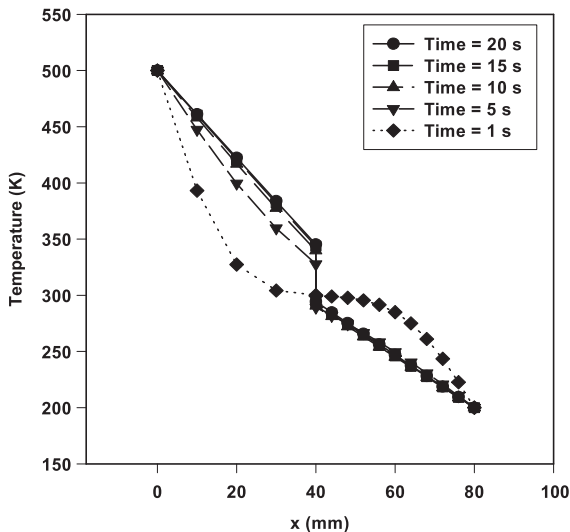
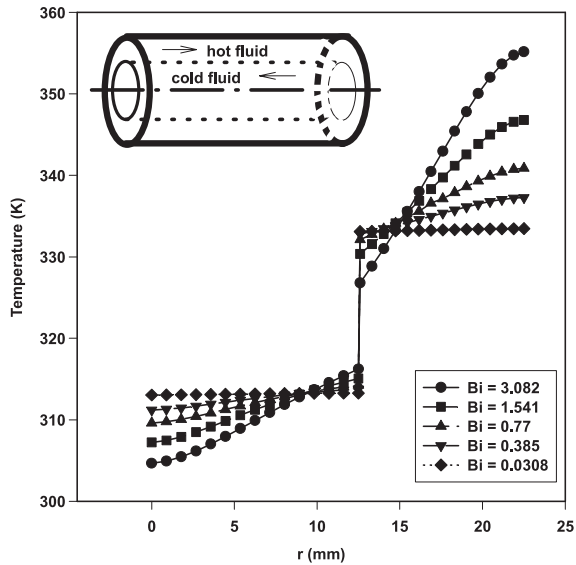


Figure 5. Transient calculations of gap heat conduction between two 3-D blocks. Parameters for computations: density (ρ) = 2330 kg/m³ and specific heat (C_p) = 712 J/kg-K for the top block and $\rho = 2702$ kg/m³ and $C_p = 903$ J/kg-K for the bottom block. Other parameters are the same as in Figure 3 and $Bi = 1.87$

heat transfer is one dimensional across the separator (Incropera and DeWitt, 1996). Numerical simulations were carried out and the calculated radial temperature distribution for the end of the hot stream is plotted in Figure 6 as a function of $Bi = hR/2k$ where R is the radius of the inner pipe. It is worth noting that $Bi = hR/2k$ is used for an axisymmetric problem as the one being considered, and for a long 2-D problem, the height of the channel should be used in place of $R/2$. The analytical solution as described in the standard textbooks assumes no thermal diffusion in the radial direction and matches well with the temperature profile with $Bi = 0.0308$ (Incropera and DeWitt, 1996; Mills, 1999). Inspection of the results shows that the radial temperature distribution is a strong function of the $Bi = hR/2k$. In fact, the larger the Bi , the more non-uniform the radial temperature distribution becomes. The numerical predictions agree with analytical solutions only when $Bi = hR/2k$ is sufficiently small. In the classical approach documented in standard textbooks, a uniform temperature distribution is tacitly assumed for heat exchanger calculations. Clearly this assumption is invalid when the Bi number is large. It is attributed to the fact that for these conditions the thermal conduction is not fast enough to dissipate heat transferred from the other moving stream. Our extensive numerical testing further suggests that the classical 1-D solution is valid only for $hR/2k < 0.1$. This conclusion is of critical importance in that in virtually all textbooks on heat exchanger designs, hR/k has never been considered as a

Figure 6.
Radial temperature distribution in a concentric heat exchanger as a function of $Bi = hR/2k$. Parameters used for computation: diameter (D) = 25 (mm), flowrate in the annulus = 0.2 Kg/s, $k = 0.625$ W/m-K, $Cp = 4178$ J/kg-K, $\rho = 1000$ kg/m³ and viscosity (μ) = 725×10^{-6} N-s/m² for the fluid in the inner pipe; and diameter (D) = 45 (mm), flowrate in the annulus = 0.1 Kg/s, $k = 0.138$ W/m-K, $Cp = 2131$ J/kg-K, $\rho = 884.1$ kg/m³ and $\mu = 3.25 \times 10^{-2}$ N-s/m² for the fluid in the annulus



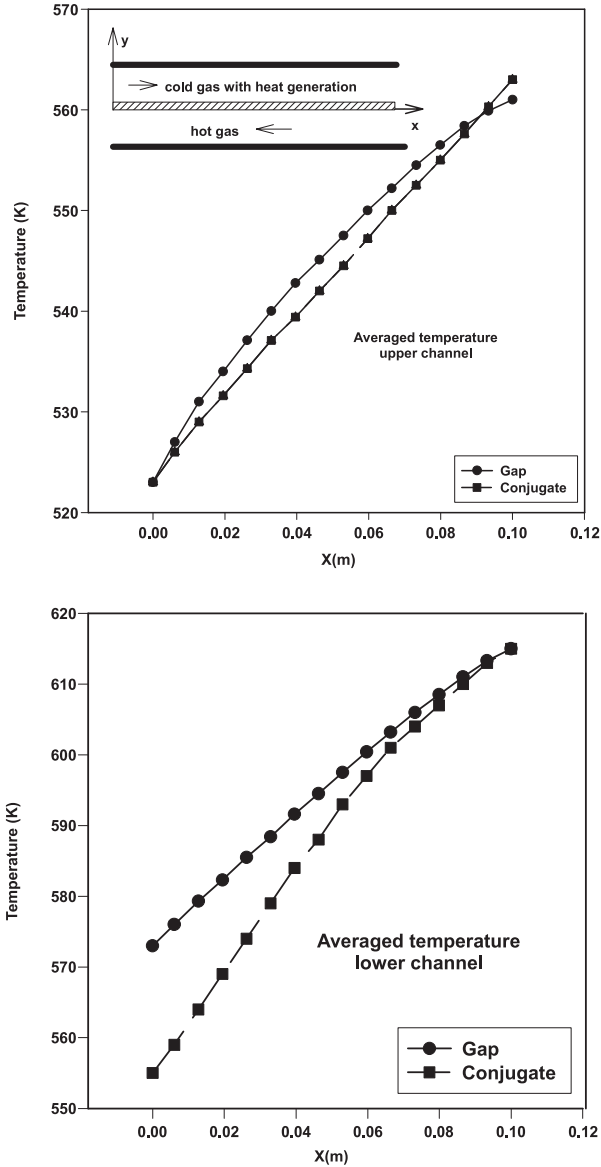
criterion. This criterion must be checked and satisfied to ensure the validity of the widely accepted 1-D analytical treatment. When this criterion is not satisfied, however, calculations employing the gap elements represent the next level of simplification and should be used if the detailed flow structure is not desired.

Microchannels involving heat release

This problem is concerned with heat transfer in a microchannel system involving chemical reaction and the problem is solved again by using both the direct numerical solution and the gap element approach. For the direct numerical solution, both detailed fluid flow and temperature distributions are calculated. The gap element calculations used the plug flow and the heat transfer coefficient was obtained using the standard convective heat transfer correlations. The averaged temperature distributions along the x -direction in both the upper and lower channels are given in Figure 7. The device is a typical design for micro fuel cell power generation and the chemical reaction rate may be simplified as a linear relation. The channel is 100 mm long and 4 mm high. The hot gas is to provide needed heat to induce the chemical reaction in the cold stream. In the calculations, the properties of mixtures were used for both streams, and gaseous species distributions due to combustion processes were not considered, because of a lack of accurate data. The results show that while the general trends in temperature distributions are predicted by both the gap element approach and direction numerical simulations, the values differ by as much as 20 percent by the two approaches. One important reason for this discrepancy comes from the fact that the heat transfer coefficient for the gap element calculations is based on the fluids with no chemical reaction. When the chemical reaction takes place, the temperature distributions become different and so is the heat flux along the solid liquid interface. With this correction taken into account, the difference becomes reasonably small, except near the solid liquid interface, as expected. Thus, for the gap elements to be useful for this type of calculations, correct heat transfer coefficients should be used. For the case where such reliable data are not available, the direct numerical simulations must be used to calculate the temperature distributions.

For this problem, computed results by both direct numerical simulations and the gap element approach were also compared with 1-D analytical solutions as given in the standard textbooks, with the chemical reaction rates set to zero. It was found that for this particular system, the axial conduction along the separator is significant. The analytical solution predicts an incorrect temperature distribution trend for both streams, even with the same heat transfer coefficient used for gap element calculations. With the axial conduction in the separator considered for the analytical solution, which results in considerable algebraic manipulations and very complex formulae, the match among all the three methods becomes gratifying.

Figure 7.
 Solution of heat transfer in a micro fuel cell reactor using the direct numerical simulation and gap element approach. The channel size: 100 mm long \times 4 mm height. The thermal properties for the hot fluid:
 $\rho = 0.6964 \text{ kg/m}^3$,
 $\mu = 270.1\text{E-}07$,
 $k = 40.7\text{E-}03 \text{ W/m-K}$,
 $C_p = 1030 \text{ J/kg-K}$, and
 that for the cold fluid:
 $\rho = 0.6521 \text{ kg/m}^3$,
 $\mu = 166.04\text{E-}07$,
 $k = 26.39\text{E-}03 \text{ W/m-K}$,
 $C_p = 2158.6 \text{ J/kg-K}$.
 $Bi = 1.793$. The volumetric heat source for chemical reaction:
 $Q = 0.731T + 1030 \text{ KJ/m}^3$.
 The properties of the separator used for direct simulations:
 $\rho = 2702 \text{ kg/m}^3$,
 $C_p = 903 \text{ J/kg-K}$,
 $k = 237 \text{ W/m-K}$ and
 thickness = 2mm



Concluding remarks

This paper has presented a finite element computational methodology for the solution of conjugate heat transfer problems with and without the use of gap elements. The finite element formulation of the conjugate heat transfer problems was presented, along with two different (i.e. direct and iterative)

methods to incorporate gap elements into a general finite element program. The advantages and disadvantages of the two gap element treatments were also discussed. The numerical performance of the iterative gap element treatment has been discussed in detail in comparison with analytical solutions for both 2- and 3-D gap conductance problems. It was found that the number of iterations depends on the non-dimensional number $Bi = hL/k$, and it increases approximately linearly with Bi for $Bi \geq 0.6$. This conclusion remains the same for both 2- and 3-D problems, for both linear and quadratic elements and for both transient and steady state calculations. Further numerical results for conjugate heat transfer problems encountered in heat exchanger and micro chemical reactors were obtained using the gap element approach, the direct numerical simulations and analytical solutions whenever solvable. The results show that for the standard heat exchanger designs, the accurate prediction of temperature distribution in the moving streams must take into consideration the radial temperature distribution and the accuracy of the calculation depends on the non-dimensional number $Bi = Rh/k$. Based on the calculations using the gap elements, it is found that $Bi < 0.1$ is required to ensure the validity of the classical analytical solutions. This important point has so far been neglected in virtually all the textbooks on heat transfer and must be included to complete the heat transfer theory for heat exchanger designs. Results also suggest that for thermal fluids systems involving chemical reactions such as micro fuel cells, the gap element approach yields accurate results only when the heat transfer coefficient exists that allows for the chemical reactions. When these heat transfer coefficients do not exist, direct numerical simulations should be used for an accurate prediction of the thermal performance of these systems.

References

- Bathe, K.J. and Chaudhary, A. (1985), "A solution method for planar and axisymmetric contact problems", *Int. J. Num. Meth. Eng.*, pp. 65–88.
- Cebeci, T. and Bradshaw, P. (1989), *Physical and Computational Aspects of Convective Heat Transfer*, Springer-Verlag, New York, NY.
- Choi, C.K. and Chung, G.T. (1996), "A gap element for three-dimensional elasto-plastic contact problems", *Computers and Structures*, Vol. 61, pp. 1155–67.
- Davis, G.V. (1983), "Natural convection in a square cavity—a benchmark solution", *Int. J. Num. Meth. In Fluids*, Vol. 3, pp. 249–64.
- Gartling, D.K. and Reddy, J.N. (1994), *Finite Element Method for Fluid Dynamics and Heat Transfer*, CRC Press, Boca Raton, FL.
- Incropera, F.P. and DeWitt, D.P. (1996), *Introduction to Heat Transfer*, 3rd ed., John Wiley & Sons, New York, NY.
- Landenberger, A. and El-Zafrany, A. (1999), "Boundary element analysis of elastic contact problems using gap finite elements", *Computers and Structures*, Vol. 71, pp. 651–61.

LeBounty, C. Shakouri, A., Robinson, G., Abraham, P. and Bowers, J. E. (1999), "Design of thin film coolers", 18th International Conference on Thermoelectrics, Baltimore, MD, pp. 273–82.

Mills, A.F. (1999), *Heat Transfer*, 2nd, Prentice Hall, Englewood Cliffs, NJ.

Narumanchi, S., Amon, C. H. and Murthy, J. (2000), "Dielectric Jet Impingement Cooling of Electronic Chips", ASME Heat Transfer Conference 2000, Pittsburgh, PA, pp. 1176–82.

Rule, T., Lynn, K. and Li, B.Q. (2000), "Finite element modeling of thermal and fluid flow phenomena in melt growth of CdTe single crystals", *Proceedings of the ASME Heat Transfer Division*, Vol. 5 No. (HTD 366-5), pp. 291–9.

Srinivas, K. and Fletcher, C.A.J. (1992), *Computational Techniques for Fluid Dynamics*, Springer-Verlag, New York, NY.

Stadler, J.T. and Weiss, R.O. (1979), "Analysis of contact through finite element gaps", *Computers and Structures*, Vol. 10, pp. 867–73.

Tannehill, J.C., Anderson, D.A. and Pletcher, R.H. (1997), *Computational Fluid Mechanics and Heat Transfer*, 2nd ed., Taylor and Francis, New York, NY.

Appendix. Interpolation of local coordinates

The interpolation procedures for obtaining geometric coordinates of points at the opposite sides of a gap element are given below for both 2- and 3-D cases, when the nodes on the two opposite sides across a gap are not geometrically coincident (Figure 2b and d).

2-D interpolation

Many algorithms may be applied to search and interpolate the corresponding points on the two opposite sides of a gap element. We present a simple and yet efficient method below, which is based on the vector dot product. Consider point $S(X_0, Y_0)$ as the integration point on one side of a gap element. To find its corresponding point at the opposite side defined by points (X_1, Y_1) and (X_2, Y_2) , two vectors V_1 and V_2 are defined as shown (Figure A1). Further, let $l = V_1 \cdot V_2$ and let L denote the length of the segment from (X_1, Y_1) to (X_2, Y_2) . Then, if $l < 0$ or $l > L$ then the projection point is out of the given segment. Otherwise, the coordinates of the projection point $P(X, Y)$ are given by the following expression:

$$X = X_1 + \frac{l}{L}(X_2 - X_1) \tag{A.1}$$

and:

$$Y = Y_1 + \frac{l}{L}(Y_2 - Y_1)$$

3-D interpolation

The interpolation procedure for 3-D problems is somewhat more involved. Again, we consider point $S(X_0, Y_0, Z_0)$ and attempts to find the corresponding point (X, Y, Z) at the opposite side of a gap element. The side is defined by four points (X_1, Y_1, Z_1) , (X_2, Y_2, Z_2) , (X_3, Y_3, Z_3) and (X_4, Y_4, Z_4) (Figure A2). Firstly, three vectors are calculated: V_1 from (X_1, Y_1, Z_1) to (X_0, Y_0, Z_0) , V_2 from (X_1, Y_1, Z_1) to (X_2, Y_2, Z_2) and V_3 is from (X_1, Y_1, Z_1) to (X_4, Y_4, Z_4) . Now, let $V = V_2 \otimes V_3$. Then, the unit normal of the plane is given by $n = V / |V|$. Let $l = V_1 \cdot n$, and l is then the length from (X_0, Y_0, Z_0) to (X, Y, Z) . Thus, the coordinates X, Y and Z are determined by:

$$X = X_0 + n_x \cdot l \tag{A.2}$$

$$Y = Y_0 + n_y \cdot l \tag{A.3}$$

$$Z = Z_0 + n_z \cdot l \tag{A.4}$$

where n_x , n_y and n_z are the components of the unit normal \mathbf{n} . To determine if the point is within the element, we calculate the areas of the four sub-triangular elements. If the sum of these areas is the same as that of the quadrilateral element, then the point is inside. Otherwise, the point is considered outside the element. An alternative is to calculate the normals of the plane of these sub-triangular elements, with point (X, Y, Z) as the first point and connecting other two points on each side of the quadrilateral in the same number sequence by which the normal \mathbf{n} is defined. If all the normals of these sub-triangular elements are the same, then the point is inside. Otherwise, it is outside.

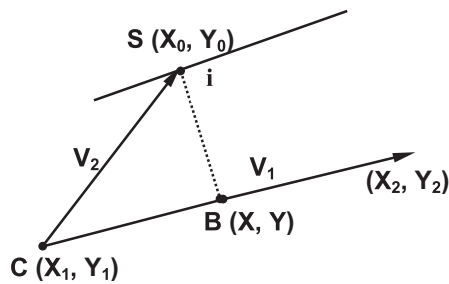


Figure A1.
Illustration of search for two points at two opposite sides for 2-D gap elements

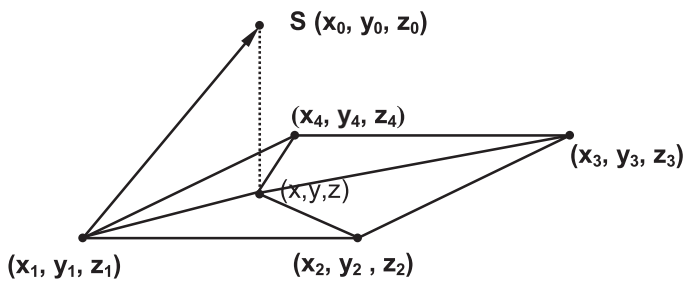


Figure A2.
Determination of two corresponding points on two opposite sides of 3-D gap elements